Available online at www.sciencedirect.com

SCIENCE DIRECT®

Journal of Catalysis 222 (2004) 461–469

JOURNAL OF CATALYSIS

www.elsevier.com/locate/jcat

Epoxidation of cyclic allylic alcohols on titania–silica aerogels studied by attenuated total reflection infrared and modulation spectroscopy

Andreas Gisler, Thomas Bürgi,[1] and Alfons Baiker *

Institute for Chemical and Bioengineering, Swiss Federal Institute of Technology, ETH Hönggerberg, CH-8093 Zürich, Switzerland

Received 21 October 2003; revised 11 December 2003; accepted 11 December 2003

Abstract

Epoxidation of cyclohex-2-en-1-ol and cyclooct-2-en-1-ol on titania–silica aerogel catalysts using *t*-butylhydroperoxide (TBHP) as oxidant was studied by in situ attenuated total reflection (ATR) Fourier transform infrared spectroscopy. Probing of the catalytic liquid–solid interface revealed different adsorption behaviors for the two allylic alcohols on the aerogel. Cyclohexenol was found to adsorb stronger and less reversible on the catalyst surface and Ti sites than cyclooctenol. The spectroscopic measurements under working conditions support the previously proposed *hydroxy-assisted* mechanism for the formation of cyclohexenol oxide and the *silanol-assisted* mechanism for cyclooctenol epoxidation. The evidence of the former is traced to the occurrence of a framework vibration upon adsorption of cyclohexenol, whereas the latter is supported by large negative bands of the silanol groups at 3700 and 980 cm^{-1} in the case of cyclooctenol epoxidation.

Keywords: Titania–silica aerogels; Epoxidation; Allylic alcohols; Attenuated total reflection infrared spectroscopy; In situ spectroscopy; Hydroxy assisted; Silanol assisted

1. Introduction

Epoxidation of functionalized olefins using Ti- and Si-based catalysts has received considerable attention in recent years [1,2]. Titania–silica aerogels belong to the catalysts which exhibit interesting catalytic potential, particular for the epoxidation of bulky functionalized olefins, mainly due to their open mesoporous structure combined with a high abundance of isolated tetrahedrally coordinated Ti sites. Most of the work aimed at elucidating the mechanism of epoxidation has been carried out on crystalline well-defined molecular sieve materials [3–9] or special homogeneous model catalysts [10–13]. Various transition-state structures have been proposed (see, e.g., [14] and references therein). However, the crystalline materials with their rigid structural constraints are generally less suitable for the epoxidation of bulky olefins [7,15]. Mechanistic studies on amorphous materials, such as titania–silica aerogels are therefore in demand and such studies must be performed under working conditions due to the metastable nature of these materials.

In the past years considerable effort has been made to further develop attenuated total reflection Fourier transform infrared (ATR-IR) spectroscopy to a versatile tool for investigating catalytic solid–liquid interfaces [16–19]. Particularly, the combination of ATR-IR with modulation spectroscopy has brought significant advantages concerning the sensitivity of the method and for the discrimination of dynamic and static surface processes [17]. In a recent study we explored the potential of the technique to study differences in the adsorptive interactions of the reactants in the epoxidation of cyclohexene [20].

Studies on the epoxidation of various allylic alcohols on titania–silica aerogels revealed striking differences in the behavior of the epoxidation depending on the allylic alcohol [14]. Particularly interesting is the difference observed when comparing the epoxidation of cyclohexenol with that of cyclooctenol. Based on the reaction rate and the highly different stereoselectivity we speculated that the different catalytic behavior can be traced to a *hydroxy-assisted* mechanism in the case of cyclohexenol epoxidation, whereas for cyclooctenol a *silanol-assisted* mechanism seems to prevail (Scheme 1).

---

* Corresponding author.

E-mail address: baiker@tech.chem.ethz.ch (A. Baiker).

[1] Present address: Institut de Chimie, Université de Neuchâtel, Switzerland.

0021-9517/$ – see front matter © 2004 Elsevier Inc. All rights reserved.
doi:10.1016/j.jcat.2003.12.009

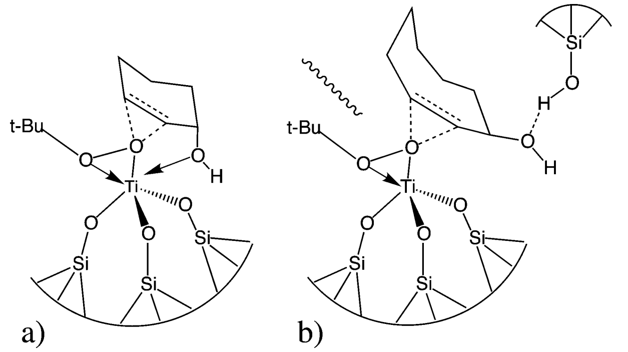

Scheme 1. Proposed transition states for the epoxidations of cyclohex-2-en-1-ol via *hydroxy-assisted* mechanism (a) and cyclooct-2-en-1-ol by a *silanol-assisted* mechanism (b). Note that different coordination for cyclooctenol may be feasible depending on the position of the neighboring silanol group.

In the present work we aim at unraveling the subtle differences in the interactions occurring during epoxidation of cyclohexenol and cyclooctenol using ATR-IR combined with modulation spectroscopy.

2. Experimental

2.1. Preparation of catalyst layer

The four aerogels used in the experiments were prepared as reported in detail elsewhere [15,21]. The catalysts were synthesized by a sol–gel process, using tetramethoxysilane (Fluka, puriss.) and titanium diisopropoxide bis(2,4-pentanedionate) (75% in i-PrOH; Aldrich puriss.) with 2-propanol (i-PrOH; Fluka, purum) as solvent, and water and HNO_3 as hydrolysant. For the aerogel modified with covalently bound methyl groups (10Ti-Me), prehydrolysis of methyltrimethoxysilane (Fluka, purum) was necessary to compensate for the different sol–gel reactivity of the precursor [22]. Trihexylamine (Fluka > 97%) was added to force gelation to an opaque monolithic body. Semicontinuous extraction with supercritical CO_2 was carried out at 40 °C and 230 bar, as described previously [23]. The as-prepared aerogel clumps were ground in a mortar and calcined in a tubular reactor with upward air flow at 400 °C. Titania–silica aerogels with 0,10, and 20 wt% nominal TiO_2 were prepared, designated 0Ti, 10Ti, and 20Ti, respectively.

The calcined aerogel was stirred in i-PrOH and the resulting slurry was dropped onto the surface of a ZnSe internal reflection element (IRE, 45°, 50 × 20 × 2 mm, KOMLAS). Subsequently, the IRE was kept at 500 Torr and 40 °C for 3 h for solvent evaporation. For achieving a uniform catalyst layer on the ZnSe IRE, this procedure had to be repeated several times. Adsorbed water and solvent were removed prior to the experiment by heating the IRE to 80 °C for 2 h at 5 Torr [20].

2.2. Nitrogen physisorption

The textural properties of the different aerogels, that is, the specific surface area (S_{BET}), mean cylindrical pore diameter, and specific desorption pore volume, assessed by the BJH method, were determined by nitrogen physisorption at $-196\,^{\circ}\mathrm{C}$ using a Micromeritics ASAP 2000 instrument. BET surface area was calculated in a relative pressure range between 0.05 and 0.2, assuming a cross-sectional area of 0.162 nm^2 for the nitrogen molecule. Pore-size distribution was calculated applying the BJH method to the desorption branch of the isotherm [24]. Maxima of pore-size distributions ($d_{\max}$) were graphically assessed from the desorption branch of the isotherms.

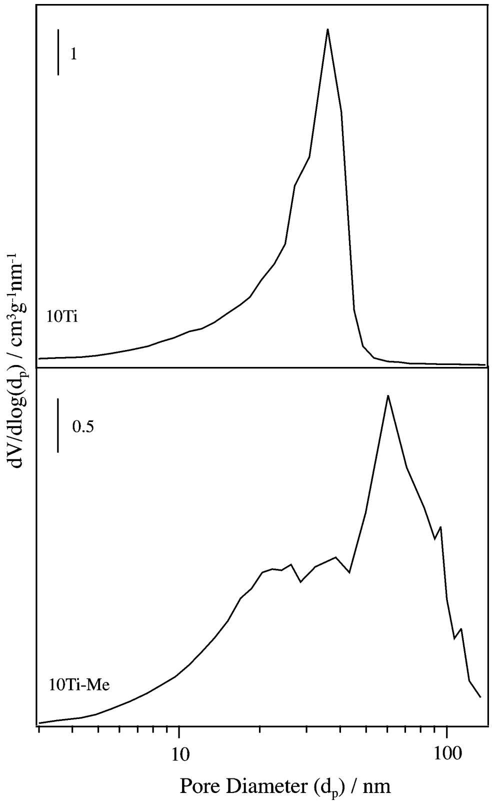

Fig. 1. Differential pore-size distributions derived from the desorption branch of the isotherm of methyl-modified titania–silica aerogel (10Ti-Me) (bottom), and the corresponding unmodified aerogel 10Ti (top). Note that the x-axis is logarithmic.

Textural properties of the aerogels (0Ti, 10Ti-Me, 10Ti, and 20Ti) were (same sequence): BET surface area, 1102, 635, 768, and 761 m^2/g; $d_{\max}$, 35, 60, 36, and 96 nm; specific pore volume, 3.77, 2.08, 2.21, and 1.46 cm^3/g.

Fig. 1 shows the differential pore-size distribution of the aerogels 10Ti and 10Ti-Me, derived from the desorption branch of the corresponding isotherms. 10Ti-Me showed the highest performance for epoxidation of cyclohexenol [21].

2.3. ATR spectroscopy

The temperature-controlled ATR flowthrough cell used for the investigations and the experimental setup were previously described in detail [17,20,25]. The cell was mounted within the sample compartment of the Fourier transform IR spectrometer (Bruker IFS-66/S) equipped with a liquid nitrogen-cooled medium band MCT (HgCdTe) photodetector. All spectra were recorded at a resolution of 4 cm^{-1} and are presented in absorbance units as $A = -\log(I/I_0)$, where I and I_0 are the reflected intensities of the sample and reference, respectively.

The flow of the reactant solutions was provided by a peristaltic pump (ISMATEC Reglo 100) and controlled by a pneumatically actuated three-way Teflon valve (PARKER PV-1-2324).

2.4. Modulation spectroscopy

The characteristic features and advantages of modulation spectroscopy have been described before [17,26]. The response of the system, stimulated by periodic variation of reactant concentration, is followed by measuring time-resolved spectra. These are converted to phase-resolved spectra by a digital phase-sensitive detection (demodulation) according to the equation:

$$A_k^{\phi_k^{\mathrm{PSD}}}(\tilde{\nu}) = \frac{2}{T}\int_0^T A(\tilde{\nu},t)\sin\bigl(k\omega t+\phi_k^{\mathrm{PSD}}\bigr)\,\mathrm{d}t,$$

$$k = 1, 2, \ldots,$$

$A(\tilde{\nu},t)$ is the time-dependent absorbance at wavenumber $\tilde{\nu}$, ω is the stimulation frequency, T is the modulation period, and ϕ_k^{PSD} is the demodulation phase angle. All spectra reported were demodulated at the fundamental frequency ($k = 1$).

The phase-sensitive detection is a narrow-band technique, which efficiently filters the noise at frequencies different from the stimulation frequency. Bands can be positive or negative, depending on the phase lag. In the following we refer to positive bands as those which are positive when the stimulation is on. A more detailed description of the technique can be found elsewhere [16,17,26–28].

2.5. Adsorption and epoxidation experiments

The procedure for adsorption and epoxidation experiments was essentially the same as previously described [20]. Typically, 60 single-beam spectra were recorded during one modulation period by averaging several scans per single beam spectrum, which were collected by coadding 40 interferograms at a rate of about 10 spectra/s. Eighteen phase-resolved absorbance spectra were calculated by varying the phase angle in 10° steps between 0 and 180°. Note that phase-resolved absorbance spectra differing by 180° are identical but for the sign of the absorbance signals.

Adsorption experiments were carried out at room temperature. Measurement of the time-resolved spectra was synchronized with the concentration modulation by switching the computer-controlled valve within the data acquisition loop. One modulation period lasted $T = 244$ s.

Epoxidation experiments with cyclooct-2-en-1-ol (97%; prepared according the procedure described by Meier et al. [29]) were carried out at 70 °C in cyclohexane (Fluka, puriss. p.a., dist. over CaH_2) solvent, and corresponding experiments with cyclohex-2-en-1-ol (Fluka, puriss. p.a.) were carried out at 80 °C in toluene (Fluka, puriss., dist. over Na). For the latter experiment, toluene was used as solvent since cyclohexane was unsuitable due to its lower boiling point (81 °C). For the concentration modulation, corresponding liquid feeds were dosed from two different tanks. Tank 1 contained a solution of allylic alcohol and *t-butyl* hydroperoxide (TBHP; Fluka, purum, $\sim$ 5.5 M in nonane) in the corresponding solvent, respectively, and tank 2 a mixture of the two reactants. Data acquisition was performed with a modulation period $T = 299$ s. Samples were collected in a time-resolved manner using a fraction collector after the cell. The samples were subsequently analyzed using a HP 6890 gas chromatograph (cool on-column injection, HP-FFAP column, 30 m × 0.32 mm × 0.25 µm).

3. Results

3.1. Adsorption experiments

Important vibrational bands of reactants and products used in this study are listed in Table 1. Fig. 2 shows ATR spectra of dissolved cyclohex-2-en-1-ol and cyclohexenol oxide in toluene as well as TBHP, cyclooct-2-en-1-ol and cyclooctenol oxide in cyclohexane ($\sim$ 10 mmol/L each) measured over the uncoated internal reflection element (IRE) in the absence of catalyst.

Table 1
Assignments of observed vibrational bands associated with reactants and products as well as catalyst framework vibrations. Bands used in discussion are in bold

Reactant/ product	Typical reactant/ product signals (cm^{-1})	Catalyst framework vibrations (cm^{-1})	Negative catalyst framework vibrations[a] (cm^{-1})
Cyclohexenol	3026, 2960, 1064, 1053, 1048, 1041, **953**, 804, 727	1035, 1027, **1020**, 1014, 1002, 983, **958**	**3700**, **980**, **890–810**
Cyclohexenol oxide	1069, 1057, 1040, 1030, 998, **944**, **931**, 864, **853**, 846	1051, **999**, 953	905–875
Cyclooctenol	3019, 2964, **1131**, 1049, 1017, 988, 962, 782, **751**, **713**	1050–1010, 990–910	**3700**, **980**, 900–780
Cyclooctenol oxide	1053, 1024, 1017, 985, 978, 970, **912**, 892, **881**, 864, 828, 821, **745**	1045, 1004, 954	850–830
TBHP	2983, 1389, **1367**, 1320, **1260**, **1250**, 1191, 844, 747	1020, 944	

[a] Signals decreasing upon exposure to concentration modulation of reactants.

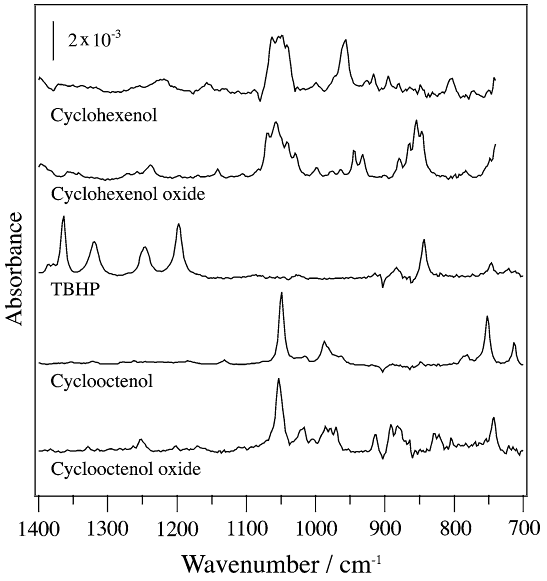

Fig. 2. Demodulated ATR spectra of reactants and products on blank internal reflection element (IRE) at room temperature: (top-down) cyclohex-2-en-1-ol, cyclohexenol oxide, *t-butyl* hydroperoxide (TBHP), cyclooct-2-en-1-ol, cyclooctenol oxide. Note that in the experiments of cyclohexenol and cyclohexenol oxide the spectral region between 730 and 700 cm^{-1} was obscured by strong absorptions of toluene used as solvent.

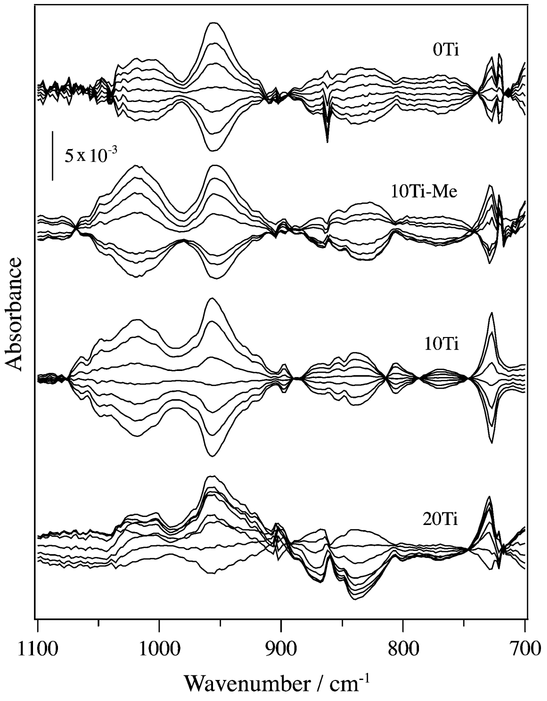

Fig. 3. Demodulated ATR spectra of adsorption of cyclohex-2-en-1-ol at room temperature on titania–silica aerogels with different Ti contents and modifications: (top-down): 0Ti ($\mathrm{SiO_2}$), methyl-modified titania–silica aerogel (10Ti-Me), 10Ti, 20Ti. The concentration of cyclohex-2-en-1-ol was modulated between 0 and 3 mmol/L in toluene.

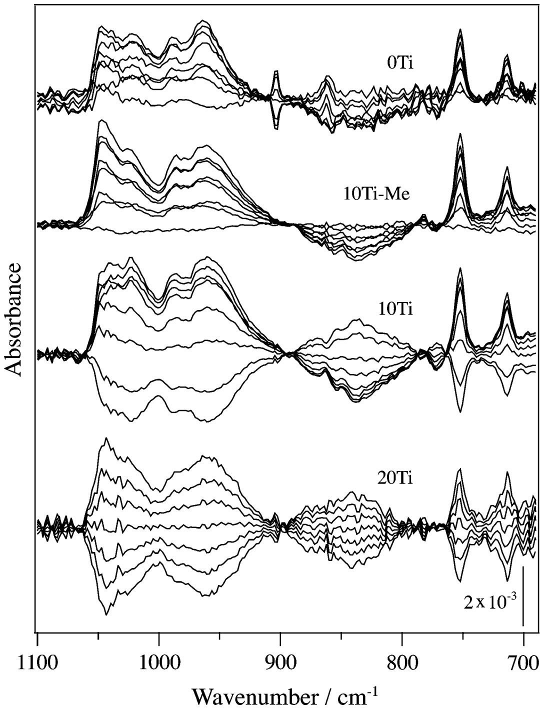

Fig. 4. Demodulated ATR spectra of adsorption of cyclooct-2-en-1-ol at room temperature on titania–silica aerogels with different Ti contents and modifications: (top-down): 0Ti ($\mathrm{SiO_2}$), methyl-modified titania–silica aerogel (10Ti-Me), 10Ti, 20Ti. The concentration of cyclooct-2-en-1-ol was modulated between 0 and 3 mmol/L in cyclohexane.

Fig. 3 shows phase-resolved ATR spectra recorded when modulating the cyclohex-2-en-1-ol concentration between 0 and 3 mmol/L at room temperature over titania–silica aerogels (0Ti, 10Ti-Me, 10Ti, and 20Ti). Prominent signals at 3026, 2960 (not shown), 1064, 1020, 1014, 1002, 953, 860, 848, 804, and 727 cm^{-1} were discernible. The negative bands at 3700 and 980 cm^{-1}, revealed a strong interaction with the surface silanol groups. The broad band at 3280 cm^{-1} indicated an interaction of the OH group of the allylic alcohol with the catalyst surface. With increasing Ti content, the area between 990 and 1080 cm^{-1} changed drastically. Note that cyclohexenol typically absorbed between 1040 and 1065 cm^{-1} (Fig. 2). Whereas for the 10Ti aerogel the signals at 1019 and 1002 cm^{-1}, as well as the typical cyclohexenol signals, became more prominent with respect to 0Ti, these bands were weaker and saturated for 20Ti. Furthermore the bands at 1027 and 1035 cm^{-1} became less intense on desorption of cyclohexenol. The broad negative band in the area between 810 and 890 cm^{-1} increased with higher Ti content, as well as the positive signals at 848 and 860 cm^{-1}. Upon initial adsorption of cyclohexenol a significant change in the framework vibration occurred giving rise to a band at 958 cm^{-1}. Note that this band is close to the C–O-stretching vibration of cyclohexenol at 953 cm^{-1}.

The corresponding adsorption experiments with cyclooct-2-en-1-ol over aerogels with different Ti content (0Ti, 10Ti-Me, 10Ti, and 20Ti) are shown in Fig. 4. Again, the concentration of the allylic alcohol was modulated between 0 and 3 mmol/L at room temperature. Typical signals could be observed at 3019, 2964 (not shown), 1049, 1017, 988, 962, 782, 751, and 713 cm^{-1}. A broad negative framework band between 900 and 780 cm^{-1} was detected, which indicates a perturbation of the symmetric Si–O–Si vibrations (see below). For all aerogels a negative band at 3700 cm^{-1} was observed. Due to overlaps with the cyclooctenol signal at 988 cm^{-1}, the corresponding negative signal of the surface silanol groups at 980 cm^{-1} is obscured. A broad signal at 3280 cm^{-1} indicated an interaction of the hydroxy group of cyclooctenol with the catalysts surface. As already observed for cyclohexenol, cyclooctenol showed a similar adsorption behavior on the methyl-modified (10Ti-Me) and the pure silica aerogel (0Ti). For these catalysts, the signals of the substrate (1048, 988, and 962 cm^{-1}) were more dominant than the signals of the framework in this area and a slight shift of the band at 1049 to 1043 cm^{-1} could be observed.

The spectra of adsorbed TBHP on the corresponding catalysts have been discussed before [20]. Typical strong bands appear at 2983, 1389, 1367, 1320, 1250 (broad), 1191, 844, and 747 cm^{-1}, which are assigned to adsorbed TBHP. The strong broad signals around 1020 and 944 cm^{-1} originate from aerogel framework vibrations.

Also, the spectrum of the 10Ti-Me catalyst was reported previously [20] and discussed in comparison with the results reported for TiO_2-SiO_2 mixed oxides by Schraml-Marth et al. [30]. Most prominent, a broad and strong band with a maximum at 1075 cm^{-1} and a shoulder at 1200 cm^{-1} could be detected, which can be assigned to the ν(Si–O–Si) asymmetric stretching vibration. The symmetric ν(Si–O–Si) stretching vibration can be found at 810 cm^{-1}. At 947 cm^{-1} a signal of the ν(Ti–O–Si) asymmetric stretching vibration could be detected, which is partially overlapped by the Si–OH vibration at 980 cm^{-1}.

3.2. *Concentration modulation experiments of epoxidation reactions*

Reactant concentration modulation experiments were performed at 80 and 70 °C, respectively, using the methyl-modified aerogel 10Ti-Me. Two different types of experiments were performed. In one the concentration of TBHP was kept constant (3 mmol/L) and the concentration of the allylic alcohol was modulated between 0 and 3 mmol/L. In the other type of experiment the allylic alcohol concentration was kept constant and the one of TBHP was modulated between 0 and 3 mmol/L. Figs. 5 and 6 show some phase-resolved ATR spectra of these experiments.

When cyclohexenol was used as reactant (Fig. 5, top), the cyclohexenol concentration modulation experiment affected the signals of surface silanols 980 cm^{-1}, while this effect was not observed for the corresponding experiment with TBHP (Fig. 5, bottom). For both experiments, no clear signals of the epoxidation product were discernible.

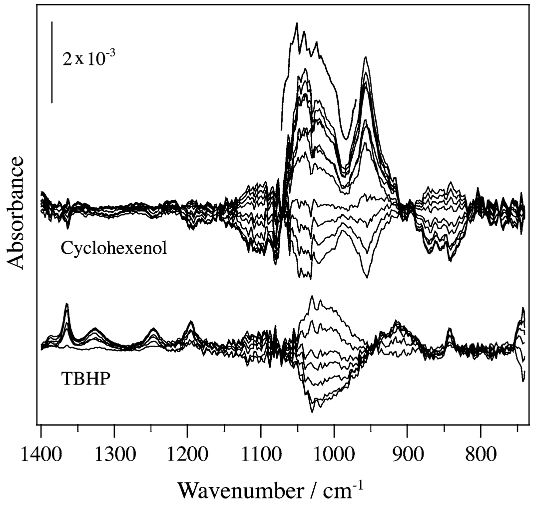

Fig. 5. Demodulated ATR spectra of epoxidation experiments recorded in the region between 1400 and 750 cm^{-1}. The concentrations of cyclohex-2-en-1-ol (top) and TBHP (bottom) were periodically modulated between 0 and 3 mmol/L in toluene at 80 °C. The topmost spectrum (1070–965 cm^{-1}) represents cyclohexenol oxide over 10Ti-Me for comparison.

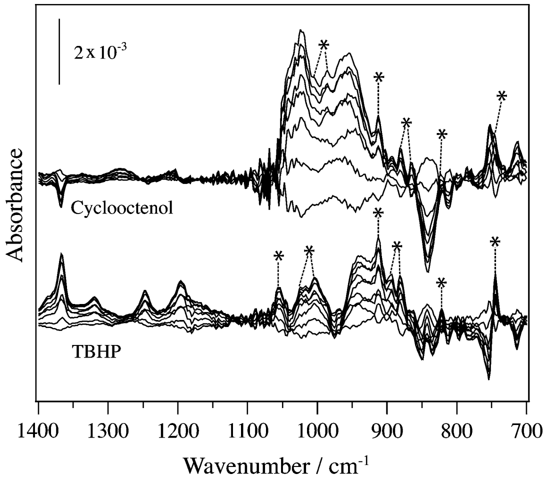

Fig. 6. Demodulated ATR spectra of epoxidation experiments recorded in the region between 1400 and 700 cm^{-1}. The concentrations of cyclooct-2-en-1-ol (top) and TBHP (bottom) were periodically modulated between 0 and 3 mmol/L in cyclohexene at 70 °C.

Only relatively weak signals could be detected between 1100 and 900 cm^{-1}, when the concentration of TBHP was modulated. While typical peroxide signals (1367, 1326, 1250, 1191, and 844 cm^{-1}) could be observed, the framework vibrations in the region between 950 and 1070 cm^{-1} were hardly influenced and exhibited a phase shift of 90° with respect to the TBHP signals. The changes in the framework vibrations typical for TBHP adsorption on the methyl-modified aerogel (10Ti-Me) at 1020 and 944 cm^{-1} could not be detected [20]. GC analysis of the effluent reaction solution showed only traces of the desired epoxide and its intensity did not seem to be periodically modulated.

In the case of cyclohexenol modulation, signals of the allylic alcohol (1064, 1053, 1048, 1041, 953, and 804 cm^{-1}) and the catalyst framework (1035, 1027, 1020, 1014, 983, and 958 cm^{-1}) could be detected. The spectrum showed a high similarity to the one of cyclohexenol adsorption on the unmodified aerogel (10Ti) at room temperature (see Fig. 3).

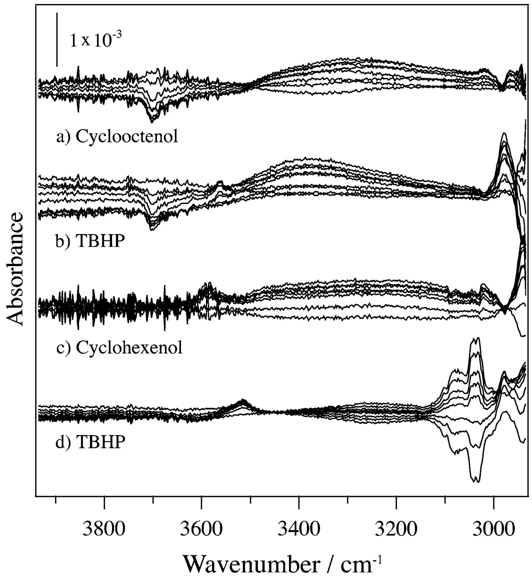

Fig. 7. Demodulated ATR spectra in the region between 3935 and 2935 cm^{-1} of epoxidation experiments of cyclohexenol (cf. Fig. 5) and cyclooctenol (cf. Fig. 6). Conditions are given in legends of Figs. 5 and 6, respectively. (Modulation of reactant concentration: (a) cyclooctenol; (b) TBHP in cyclooctenol epoxidation; (c) cyclohexenol; (d) TBHP in cyclohexenol epoxidation.)

Furthermore, negative bands at 1367, 1250, 1191, 844, and 747 cm^{-1} indicate a displacement of TBHP. Analysis of the cell effluent by GC revealed a small concentration of cyclohexenol oxide, which was, however, higher than in the TBHP modulation experiment. Yet, the concentration showed only slight periodic time dependence.

Modulation experiments using cyclooctenol as reactant revealed an interaction with surface silanol groups for TBHP as well as for the allylic alcohol. In contrast to the behavior observed with cyclohexenol, the spectra revealed negative signals at 980 and most prominently at 3700 cm^{-1}, as shown in Fig. 7. The spectra of both experiments showed the formation of cyclooctenol oxide. The signals indicated with an asterisk in Fig. 6 are associated with the epoxidation product and could also be found in the spectrum of dissolved cyclooctenol oxide. Prominent cyclooctenol oxide signals were found at 1045, 1024, 1004, 985, 970, 912, 892, 881, 864, 821, and 745 cm^{-1}. The appearance of product demonstrates that the catalyst is active under the applied conditions and the infrared spectra were recorded truly in situ. Note that the cyclooctenol oxide signal at 745 cm^{-1} partially overlaps with TBHP (747 cm^{-1}) and cyclooctenol (751 cm^{-1}) signals. Simultaneous gas chromatographic analyses of the samples taken from the cell effluents at different phase angles, as presented in Fig. 8, confirmed the formation of cyclooctenol oxide.

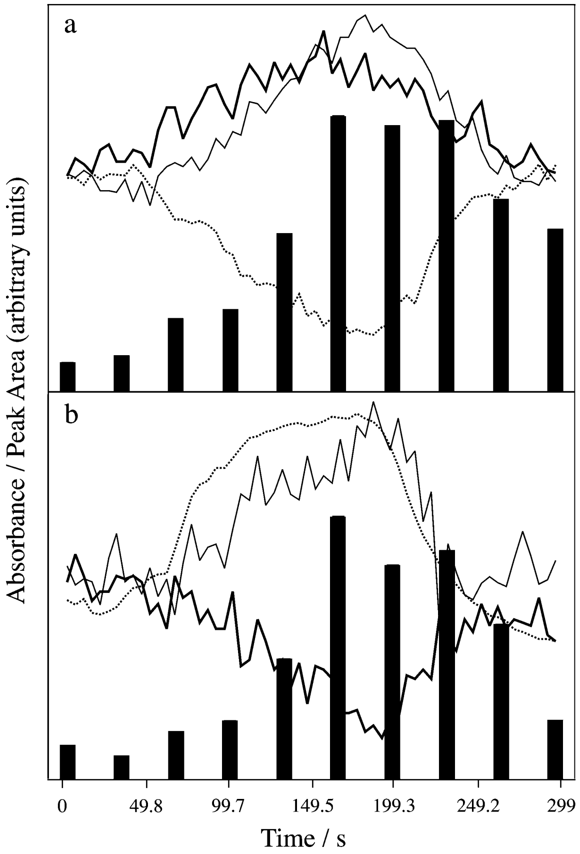

Fig. 8. Time dependence of signals for the experiments shown in Fig. 6. (a) Modulation of cyclooctenol concentration and (b) modulation of TBHP concentration. Change of *trans*-cyclooctenol oxide concentration analyzed by GC (pillars). Intensities of the cyclooctenol oxide signal at 912 cm^{-1} (thin line) and corresponding reactants (bold line, cyclooctenol at 713 cm^{-1}; dotted line, TBHP at 1396 cm^{-1}) in the time-resolved IR spectra.

When the TBHP concentration was modulated (Fig. 6, bottom), the typical signals for the adsorption of the peroxide on the catalyst could be observed (1367, 1320, 1250, 1191, 1020, 944, and 844 cm^{-1}). Interestingly, additional signals at 1260 and at 936 cm^{-1} were observed, which hinted to adsorption on the active sites [20]. The negative bands at 753 and 713 cm^{-1} are indicative for cyclooctenol desorption from the catalyst. Reactants, activated species, and product showed different phase lags. The cyclooctenol signal at 713 cm^{-1} reached its minimum at 70° demodulation phase angle, while the TBHP signal at 1367 cm^{-1} had its maximum at 100°. The signal originating from the peroxide adsorbed on the Ti site (1260 cm^{-1}) reached its maximum at 30° and the one for the cyclooctenol oxide signal at 881 cm^{-1} was observed at 60°. Spectra recorded before starting the modulation experiment showed a slight increase of the silanol bands at 3700 and 980 cm^{-1} before they decreased again when TBHP concentration was raised. The scans were recorded starting at the steady state, when the allylic alcohol in cyclohexane was flown through the cell and before the peroxide was applied for the first time.

For the corresponding epoxidation experiment with cyclooctenol concentration modulation (Fig. 6, top), the characteristic framework bands in the area between 1050 and 940 cm^{-1} and the signals of the allylic alcohol at 753 and 713 cm^{-1} were observed, as for the adsorption experiments. The negative signals at 2983, 1367, 1250, 1191, and

844 cm^{-1} indicate a desorption of TBHP. Note that for both epoxidation experiments, the signal at 844 cm^{-1} overlaps with the broad negative framework band between 900 and 780 cm^{-1}. Also in this case, the various compounds exhibit a different phase lag. The maximum of the cyclooctenol signal at 713 cm^{-1} appears at 80° demodulation phase angle while the one of the TBHP signal (1367 cm^{-1}) can be observed at 50°. The epoxide signal at 881 cm^{-1} reaches its maximum at 180°.

4. Discussion

As noted in the Introduction, comparative studies of the epoxidation of various allylic alcohols on aerogels with a Ti content of 1 and 5 wt% using TBHP as oxidant showed remarkable differences in reactivity and regio- and stereoselectivity depending on the allylic alcohol [14]. In particular vastly different rates as well as chemoselectivity and stereoselectivity were observed for the epoxidation of cyclooctenol and cyclohexenol. The turnover numbers (TON) for 2 min (7.2 and 1.4, respectively) and 2 h (39.5 and 10.2, respectively) as well as the times necessary for 50% TBHP conversion (8 and 56 min, respectively) showed a higher reactivity for cyclooctenol. On the other hand, the diastereoselectivity for *cis*-epoxide was much higher in the case of cyclohexenol (82.5 and 14.5%, respectively). The present spectroscopic investigations provide substantial evidence for the earlier speculations made that in the case of the cyclohexenol a hydroxy-assisted interaction prevails, whereas for the cyclooctenol epoxidation a silanol-assisted interaction is dominant, due to steric hindrance (Scheme 1).

The cyclohexenol adsorption experiments (Fig. 3) reveal a strong adsorption on the surface of the different catalysts, which can clearly be seen by the negative signals at 3700 and 980 cm^{-1}, indicating a strong binding to the surface silanol groups. Since the prominent signal at 1020 cm^{-1} is absent for the adsorption on the pure silica aerogel (0Ti), this band seems to be originating from framework vibrations which are influenced by the Ti sites. The saturation of typical cyclohexenol signals (1064–1041 cm^{-1}) for the aerogel with 20 wt% nominal TiO_2 (20Ti) indicates an irreversible adsorption on the catalyst. On the other hand, the appearance of a stronger negative band between 890 and 810 cm^{-1} for this catalyst also points to a strong but reversible interaction with the catalyst framework, thus revealing different adsorption behavior on different sites of the catalyst. A second prominent signal next to the typical cyclohexenol band at 953 cm^{-1} appears at 958 cm^{-1} for the adsorption on the catalysts 10Ti and 20Ti. This corroborates the assumption of an interaction with the active site, since a similar behavior could be found for adsorption of TBHP [20].

When cyclooctenol is adsorbed on the catalysts, the spectra reveal an interaction of the surface silanols with the hydroxy group of the allylic alcohol (Fig. 4). For the 10Ti and 20Ti aerogels, these interactions seem to be stronger than for the other two catalysts, which can be seen by the higher intensity of the negative band at 3700 cm^{-1}. Also, the framework vibrations seem to have bigger influence on the ATR spectra which underlines the assumption of a stronger interaction between cyclooctenol and these catalysts. For 10Ti-Me and 0Ti aerogels on the other hand, the signals of cyclooctenol seems to be stronger, for example, a weak signal at 1131 cm^{-1} (not shown) can only be observed for these two catalysts. This hints to more reversible adsorption and desorption of cyclooctenol on these catalysts with consequently less saturation of the signals. The molecules appearing at the interface therefore dominate the spectra. Compared to the adsorption experiments with cyclohexenol, cyclooctenol seems to have a more reversible and weaker interaction with all catalysts.

In the epoxidation experiments the difference of the adsorption becomes more obvious. When the TBHP concentration is modulated in the epoxidation of cyclohexenol (Fig. 5, bottom), the observations reveal a stronger adsorption of cyclohexenol on the surface and the active sites compared to TBHP. The lack of negative signals originating from the allylic alcohol (e.g., 953 or 727 cm^{-1}) and typical framework bands observed for TBHP adsorption (1020 and 944 cm^{-1}) indicate that the catalyst remains mainly static when TBHP concentration is modulated. Hence, no significant displacement of cyclohexenol by TBHP could be detected, except when the peroxide was flown through the cell for a very long period. Even interaction with surface silanol groups could not be detected. Interestingly, the framework vibrations seem to react with a delay to the appearance of TBHP on the surface, which corroborates the hindrance of TBHP adsorption by cyclohexenol. Therefore, it is not surprising that no cyclohexenol oxide could be detected in the spectra and only traces were discernible in the GC analysis. When modulating the concentration of cyclohexenol (Fig. 5, top), the typical spectrum of the allylic alcohol can clearly be observed. Furthermore the negative bands of TBHP indicate a displacement of the peroxide. This clearly shows a stronger adsorption on the catalyst for cyclohexenol with respect to TBHP. Since this experiment showed a higher concentration of cyclohexenol oxide in the effluent solution and its intensity even marked a slight dependence on the cyclohexenol concentration, the shoulder at 999 cm^{-1} and the weak signals at 944, 931, and 853 cm^{-1} may indicate cyclohexenol oxide formation. This is strongly supported by the topmost spectrum (bold) in the range between 1070 and 965 cm^{-1} of cyclohexenol oxide over 10Ti-Me (Fig. 5, top). Interestingly, when the experiment was repeated 5 min later, the ATR spectrum revealed a clear deactivation since both the cyclohexenol signals and the negative TBHP bands were much weaker (Fig. 9). Fig. 9 shows that in the second experiment the bands are in general much weaker. As only dynamic changes are visible in the demodulated spectra the comparison in Fig. 9 shows that in the second experiments the catalyst was less active. This corroborates the findings of Beck et al. [14] who observed a fast catalyst deactivation

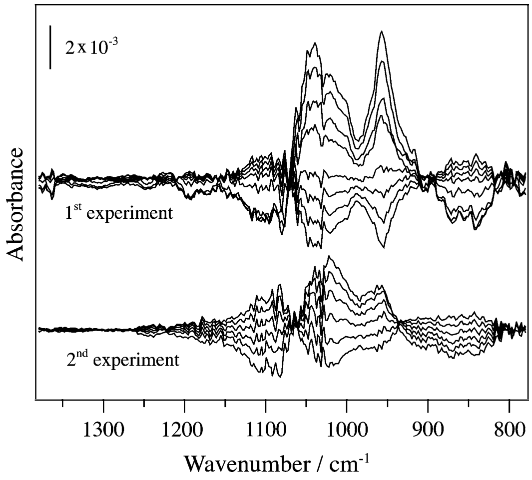

Fig. 9. Demodulated ATR spectra of epoxidation experiments recorded in the region between 1380 and 780 cm^{-1}. The concentration of cyclohex-2-en-1-ol was periodically modulated between 0 and 3 mmol/L in toluene at 80 °C. The second experiment (bottom) was started 5 min after the first experiment (top) was finished.

for the epoxidation of cyclohexenol. They also suggested that the allylic alcohol blocks the active sites and therefore deactivates the catalyst. This is fully supported by our experiments described above and also by variable temperature experiments where the catalyst was slowly heated. GC analysis of the effluent reaction solution showed the highest concentration of cyclohexenol oxide at 75 °C, although best performances were reported for 90 °C [21].

In the case of cyclooctenol epoxidation, the adsorption behavior of the allylic alcohol plays a different role. When the TBHP concentration was modulated (Fig. 6, bottom), a displacement of cyclooctenol could clearly be monitored by the two negative bands at 751 and 713 cm^{-1}. The negative bands of the silanol groups at 3700 and 980 cm^{-1} and the signal at 1260 originating from TBHP coordinating to the active Ti site [20] indicate a weaker adsorption of the allylic alcohol on the catalyst surface and active sites than observed for cyclohexenol. When investigating the scans taken before starting the epoxidation experiment, it can clearly be observed that the silanol signal at 3700 cm^{-1} increased before decreasing again when TBHP concentration is raised (vide infra). This indicates a desorption of cyclooctenol before TBHP adsorbs on the surface silanols. Therefore coordination and activation of the peroxide at the Ti active sites are possible and the formation of the epoxide is evident. GC analysis showed a clear periodic increase and decrease of cyclooctenol oxide concentration. The phase lag of 110° for the two TBHP signals at 1250 and 1260 cm^{-1} reveals the rate-determining factor. Since the first band indicates the adsorption on the surface silanol groups and the latter the adsorption at the Ti centers, the phase lag reflects the time needed for the pore diffusion and/or coordination to the active site. The phase lag for the TBHP signal at 1250 cm^{-1} and the cyclooctenol oxide signal at 881 cm^{-1} is 140°, which is smaller than that found for the epoxidation with cyclohexene (180°) [20].

Modulation of the cyclooctenol concentration reveals a strong adsorption on the catalyst and a displacement of TBHP not only by consumption of the latter on the active sites (Fig. 6, top), but also on the residual surface. The strong negative band at 3700 cm^{-1} indicates adsorption of cyclooctenol on the catalyst surface via silanol groups. Note that in the corresponding experiment using cyclohexene as substrate, this band was not discernible due to the weak interaction with the catalyst surface and the blocking of the silanol sites by TBHP [20]. The phase lag for the cyclooctenol signal at 713 cm^{-1} and the one of the epoxide at 881 cm^{-1} is 90° and therefore smaller than the corresponding phase lag observed for the TBHP concentration modulation. This is probably due to the fact that TBHP is already coordinated to the Ti site and therefore can react with the allylic alcohol as soon as the latter is adsorbed on the active site.

Compared to the experiment with cyclohexene, where the observed phase lag was 150° [20], the cyclooctenol oxide seems to be formed faster once the allylic alcohol is detected on the surface. This may be surprising at first glance, since cyclohexene has a smaller Van der Waals radius than cyclooctenol and, most important, does not reveal any strong interaction with the catalysts surface. Hence the olefin should diffuse more rapidly into the pores, resulting in shorter traveling time from the catalyst surface to the active site [20,31]. Using an aerogel with 5 wt% nominal TiO_2, Beck et al. found higher TONs for cyclooctenol than for cyclohexene, for a reaction time of 2 min as well as for 2 h [14]. The faster formation of the cyclooctenol oxide may be traced to the dominance of a silanol-assisted epoxidation mechanism where the allylic alcohol adsorbs on a surface silanol group adjacent to the Ti site or vicinal to it (Scheme 1) [8, 32–34].

In the case of cyclohexenol, the dative bond of the oxygen of the allylic alcohol to the active site as described by Kumar et al. for TS-1 [6] is much stronger mainly due to the smaller steric demand of the molecule compared to cyclooctenol.

Our experiments revealed catalyst deactivation and reduced accessibility for TBHP on the surface and the active site in the case of cyclohexenol, which explains the slower formation of cyclohexenol oxide. The prevalence of the hydroxy-assisted mechanism for cyclohexenol epoxidation is also indicated by the stereoselectivity of the formed epoxide. GC analysis of the effluent solution revealed formation of *cis*-cyclohexenol oxide as the main product, whereas with cyclooctenol mainly the *trans*-epoxide was observed. A close and dative bonding to the Ti site leads to a hydroxy-assisted epoxidation mechanism which favors the formation of a *cis*-epoxide.

5. Conclusions

ATR infrared combined with modulation spectroscopy in a flowthrough cell was used to study the interaction of cyclohex-2-en-1-ol and cyclooct-2-en-1-ol with TiO_2–SiO_2 aerogel catalysts as well as the epoxidation of the two allylic alcohols by *tert-butyl* hydroperoxide. The phase-sensitive detection afforded an enhanced sensitivity which is required to study the relevant small changes due to the periodic perturbation of this catalytic system by forced concentration modulation. For both allylic alcohols interaction with surface silanol groups and Ti sites could be observed. Cyclohexenol revealed a stronger and less reversible adsorption on aerogels compared to cyclooctenol. No displacement of cyclohexenol was observed when the peroxide concentration was modulated, whereas TBHP desorption could be observed when the concentration of the allylic alcohol was changed. The strong and irreversible adsorption of cyclohexenol leads to catalyst deactivation by blocking the active Ti sites. When cyclooctenol was used as substrate, epoxide formation could clearly be observed. Modulating the TBHP concentration revealed a clear displacement of the allylic alcohol. Even activation of the peroxide by coordination at the active site was discernible. A time (phase) lag between the appearance of reactant and product in the volume probed by the evanescent field was observed. The main part of this phase lag is caused by diffusion and/or adsorption of TBHP at the active site. When the cyclooctenol concentration was modulated, a displacement of peroxide was discernible. Also, a phase lag between the appearance of substrate and epoxide was observed, which was smaller than in the experiment where the TBHP concentration was modulated.

Interaction of the hydroxy group of cyclohexenol with the active site is very strong and therefore mainly *cis*-epoxide is formed. For the cyclooctenol, the interaction of the hydroxy group with Ti sites plays a less important role in the epoxidation process, due to steric hindrance. Interaction with silanol groups adjacent to the active Ti sites is favored which leads to the *trans*-epoxide as the main product.

References

[1] X.T. Gao, I.E. Wachs, Catal. Today 51 (1999) 233.
[2] M. Dusi, T. Mallat, A. Baiker, Catal. Rev. Sci. Eng. 42 (2000) 213.
[3] H.C.L. Abbenhuis, S. Krijnen, R.A. van Santen, Chem. Commun. (1997) 331.
[4] B. Notari, Stud. Surf. Sci. Catal. 37 (1988) 413.
[5] G.L. Marra, G. Artioli, A.N. Fitch, M. Milanesio, C. Lamberti, Micropor. Mesopor. Mater. 40 (2000) 85.
[6] R. Kumar, G.C.G. Pais, B. Pandey, P. Kumar, J. Chem. Soc., Chem. Commun. (1995) 1315.
[7] W. Adam, A. Corma, T.I. Reddy, M. Renz, J. Org. Chem. 62 (1997) 3631.
[8] D. Gleeson, G. Sankar, C.R.A. Catlow, J.M. Thomas, G. Spano, S. Bordiga, A. Zecchina, C. Lamberti, Phys. Chem. Chem. Phys. 2 (2000) 4812.
[9] P.E. Sinclair, C.R.A. Carlow, J. Phys. Chem. B 103 (1999) 1084.
[10] P.G. Potvin, P.C.C. Kwong, M.A. Brook, J. Chem. Soc., Chem. Commun. (1988) 773.
[11] K.B. Sharpless, S.S. Woodard, M.G. Finn, Pure Appl. Chem. 55 (1983) 1823.
[12] K.A. Jørgensen, R.A. Wheeler, R. Hoffmann, J. Am. Chem. Soc. 109 (1987) 3240.
[13] C. Beck, T. Mallat, A. Baiker, New J. Chem. 27 (2003) 1284.
[14] C. Beck, T. Mallat, A. Baiker, Catal. Lett. 88 (2003) 203.
[15] R. Hutter, D.C.M. Dutoit, T. Mallat, M. Schneider, A. Baiker, J. Chem. Soc., Chem. Commun. (1995) 163.
[16] D. Baurecht, U.P. Fringeli, Rev. Sci. Instrum. 72 (2001) 3782.
[17] T. Bürgi, A. Baiker, J. Phys. Chem. B 106 (2002) 10649.
[18] D. Ferri, T. Bürgi, J. Am. Chem. Soc. 123 (2001) 12074.
[19] D. Ferri, T. Bürgi, A. Baiker, J. Phys. Chem. B 105 (2001) 3187.
[20] A. Gisler, T. Bürgi, A. Baiker, Phys. Chem. Chem. Phys. 5 (2003) 3539.
[21] C.A. Müller, M. Maciejewski, T. Mallat, A. Baiker, J. Catal. 184 (1999) 280.
[22] C.J. Brinker, G.W. Scherer, Sol–Gel Science, Academic Press, Boston, 1990.
[23] D.C.M. Dutoit, M. Schneider, A. Baiker, J. Catal. 153 (1995) 165.
[24] J.C.P. Broekhoff, Preparation of Heterogeneus Catalysts II, Elsevier, Amsterdam, 1979.
[25] D. Ferri, T. Bürgi, A. Baiker, Helv. Chim. Acta 85 (2002) 3639.
[26] R. Wirz, T. Bürgi, A. Baiker, Langmuir 19 (2003) 785.
[27] M. Müller, R. Buchet, U.P. Fringeli, J. Phys. Chem. 100 (1996) 10810.
[28] U.P. Fringeli, D. Baurecht, M. Siam, G. Reiter, M. Schwarzott, T. Bürgi, P. Brüesch, in: H.S. Nalwa (Ed.), Handbook of Thin Film Materials, vol. 2, Academic Press, New York, 2001, p. 191.
[29] H. Meier, C. Antony-Mayer, C. Schulz-Popitz, G. Zerban, Liebigs Ann. Chem. (1987) 1087.
[30] M. Schraml-Marth, K.L. Walther, A. Wokaun, B.E. Handy, A. Baiker, J. Non-Cryst. Solids 143 (1992) 93.
[31] D. Rivera, J.M. Harris, Anal. Chem. 73 (2001) 411.
[32] M.C. Klunduk, T. Maschmeyer, J.M. Thomas, B.F.G. Johnson, Chem. Eur. J. 5 (1999) 1481.
[33] T. Maschmeyer, M.C. Klunduk, C.M. Martin, D.S. Shephard, J.M. Thomas, B.F.G. Johnson, Chem. Commun. (1997) 1847.
[34] M. Crocker, R.H.M. Herold, A.G. Orpen, M.T.A. Overgaag, Chem. Soc., Dalton Trans. (1999) 3791.